# Electronic excitations of poly(methylphenylsilane) films

R. G. Kepler
*Sandia National Laboratories, Albuquerque, New Mexico 87185*

Z. G. Soos
*Department of Chemistry, Princeton University, Princeton, New Jersey 08544*
(Received 26 December 1990)

We report electroabsorption (EA), two-photon absorption (TPA), and the spectrum for charge-carrier generation in thin films of poly(methylphenylsilane) (PMPS). The one-photon absorption to a singlet exciton, which begins at $E_g = 3.5$ eV, appears in EA and indicates a polarizability change of $1.8 \times 10^{-22}$ cm$^3$. The onset around 4.6 eV of direct generation of charge carriers by photons defines the interband gap $E_b$ and correlates with an EA feature at 4.65 eV that we associate with charge transfer between polymer segments. The TPA around 4.4 eV is to the second $^1A_g$ state and gives the alternation gap $E_a$, while the broad TPA above 5 eV is assigned to an even-parity state derived from exciting two electrons across $E_g$. A Pariser-Parr-Pople model for $\sigma$ conjugation in polysilanes accounts for $E_g$, for polarizability changes, for TPA, and for the singlet-triplet gap $E_t$ in terms of correlated states. We contrast the spectra of amorphous PMPS with films of poly(di-*n*-hexylsilane), whose side groups are ordered at low temperature, and compare EA spectra in polysilanes with EA in crystalline organic solids and wideband semiconductors.

## I. INTRODUCTION

Conjugated polymers have been intensively investigated in recent years.[1-4] In addition to the desire to understand the fundamental physics of electronic states in one-dimensional systems, a wide variety of potential applications have been identified. Early work focused on phenomena pertinent to possible uses as conductors and battery electrodes. More recently the focus has been on nonlinear optical (NLO) properties. Very large NLO coefficients have been observed and organic materials may well be the materials of choice for many NLO applications.[5] Such applications presuppose an understanding of the electronic excitations, including high-energy states that contribute to NLO coefficients.

Conjugated polymers resemble both organic molecular solids with van der Waals contacts between chains and one-dimensional semiconductors with bandwidth $4|t| \sim 10$ eV along the backbone. Triplet, singlet, and charge-transfer (CT) excitons characterize the electronic excitations of organic molecular solids.[6] By contrast, the optical gap between the valence and conduction bands often suffices for inorganic semiconductors. The identification of excitonic and interband transitions in conjugated polymers is a current problem, although much has been learned about self-localized gap states.[7] NLO spectroscopies provide complementary information to the linear spectrum, as shown below for the polymer poly(methylphenylsilane). Two-photon absorption (TPA) identifies even-parity excitations in centrosymmetric systems, while electroabsorption (EA) identifies states with CT or interband character and even-parity excitations. Photoconduction and phosphorescence fix the excitation energy for charge carriers and triplet excitons, respectively.

Most studies of conjugated polymers have been on $\pi$-conjugated systems, notably on polyacetylene (PA), polydiacetylenes (PDA), polythiophenes (PT), among many others. Similar electronic properties have been recognized recently in $\sigma$-conjugated polymers, particularly the polysilanes, $(RR'\mathrm{Si})_n$. Each Si contributes two $sp^3$ orbitals to the half-filled $\sigma$ band, while $R$ and $R'$ are either aliphatic or aromatic side groups that, to a first approximation, do not participate in the conjugation. In addition to potential applications, polysilanes may be important for understanding the electronic structure of conjugated polymers, by providing larger alternation $t(1\pm\delta)$ along the backbone than found in $\pi$-conjugated systems. The band gap is $4|t|\delta$ in one-electron theory, with $\delta \sim 0.1$ for partial single and multiple bonds in PA, PDA, or PT and $\delta \sim 0.33$ for vicinal and geminal $sp^3$-$sp^3$ overlaps in $(\mathrm{Si})_n$. The interplay of alternation and correlation gaps is an important aspect of more realistic theoretical models that include electron-electron ($e$-$e$) correlations.[8]

Extensive studies of the optical properties of polysilanes in solution[9] have generally been understood in terms of a fairly simple model. The polymeric strands are very long, consisting typically of a chain of 10 000 silicon atoms. Each strand behaves like a collection of short, ordered segments on the order of 20 silicon atoms long, separated by conformational defects.[10] The number of defects depends on both temperature and side groups. The electronic states of the segments are then determined within the Hückel approximation using the Sandorfy $C$ method[11] with the alternating transfer integrals $t(1\pm\delta)$ along the $(\mathrm{Si})_n$ chain. Alternatively, the linear absorption of each segment can be modeled in terms of Frenkel excitons[12] corresponding to an excited $\sigma$ bond or in terms of coupled Frenkel and charge-transfer excitons.[13,14]

Using this type of model and a microscopic statistical

 

mechanical theory, Schweizer[15] successfully fit the temperature dependence of the absorption spectrum as well as the solvent dependence of the order-disorder transition temperature observed in some polysilanes. Elschner *et al.*[16] have recently shown that the disorder produced by variations in segment lengths suffices for modeling both singlet-exciton and charge-carrier dynamics. Negligibly small Stokes shifts[16,17] are rationalized in terms of electronic delocalization. The broad absorption and narrow fluorescence indicate excitation transfer between segments.

These studies focus on the static and dynamic consequences of a distribution of segment lengths. The electronic structure of individual segments is a related but separate issue. Thorne *et al.*[14] observed a strong two-photon absorption in poly(di-*n*-hexylsilane) (PDHS) 0.9 eV above the first strongly allowed one-photon transition at about 3.4 eV. Soos and Hayden[8] extended the Sandorfy *C* model of alternating transfer integrals $t(1\pm\delta)$ for $\sigma$ conjugation in silane polymers to include Coulomb interactions in the Pariser-Parr-Pople (PPP) model. The TPA is to the second $^1A_g$ state and defines the alternation gap $E_a$. Another even-parity state around 5.5 eV has been observed in PDHS via TPA,[18] photoinduced absorption,[14] and electroabsorption,[19] in agreement with the PPP model. The identification of different excitations of $(Si)_n$ segments requires further work, quite aside from the subsequent effects of a segment distribution.

In this paper we study the electronic states of solid films of poly(methylphenylsilane) (PMPS), a Si backbone polymer which has a phenyl and a methyl group attached to each Si. These films are amorphous, in contrast to crystalline PDHS. Kepler *et al.*[20] showed PMPS films to be excellent photoconductors. The first optically allowed transition is a singlet exciton, similar to Frenkel excitons in organic molecular crystals.[21,22] Abkowitz, Rice, and Stolka[23] have shown that hole transport in these films is very similar to transport in molecularly doped polymers in which it has been shown that the holes basically hop between dopant molecules.

We summarize in Sec. II the measurements of photoconduction, TPA, and electroabsorption of PMPS films. Results are presented in Sec. III. The interband gap $E_b=4.6$ eV is obtained from the photoconductivity. The EA spectrum shows both $E_g$ and $E_b$ features. The TPA spectrum places the alternation gap near $E_a=4.4$ eV and shows a stronger feature above 5 eV that is derived in PPP models from two-electron excitation at $E_g$. In Sec. IV we discuss the significance of the results and their relationship to some prior results and then summarize in Sec. V. Some of the results presented in this paper have been published previously in preliminary reports.[24–26]

## II. EXPERIMENT

The PMPS used in these experiments was provided by Zeigler and prepared by his technique.[27] For the photoconductivity experiments, samples were prepared by casting from a toluene solution onto an uv quartz substrate which had been coated with a vacuum-evaporated, semitransparent aluminum film. An aluminum electrode about 10 mm in diameter was then evaporated on top of the polymer film. Samples for the EA experiments were prepared by spin casting from a toluene solution onto a quartz substrate onto which a 7.5-nm layer of aluminum had been vacuum deposited. Another 7.5-nm aluminum electrode of total area 0.19 $cm^2$ was then vacuum deposited on top of the polymer film. Gold pads, approximately 100 nm thick, were subsequently deposited onto small areas of each electrode to allow mechanical contact with gold wires. For the TPA experiments no electrodes were required and samples were solvent cast directly onto uv quartz substrates.

For all the experiments the samples were mounted on a cold finger in a vacuum, either in a closed cycle refrigerator system or a homemade low-temperature cell.

The light source for the photoconductivity and the TPA experiments was a Nd:YAG-laser-pumped (where YAG denotes yttrium aluminum garnet) dye laser with a pulse width of about 5 ns. For the photoconductivity experiments, which were standard time-of-flight experiments, the light was incident on the sample through the quartz substrate and the semitransparent aluminum electrode. The number of carriers generated by a single pulse of light was determined by measuring the amount of charge displaced on the electrodes and the number of photons incident on the sample was determined by measuring the energy in the light pulse by reflecting a known fraction of the beam into a detector.

For the EA experiment, the light source was a high-pressure xenon arc and the light was passed through a monochromater with a spectral resolution of 0.06 nm. The intensity of the light transmitted by the sample and the two electrodes was measured with a photomultiplier, preamplifier, electrometer combination and the modulation of the transmitted light intensity induced by an applied electric field was measured with a lock-in amplifier. The sample capacitance between the two electrodes was measured to be 22.5 nf. With samples that were not used for photoconductivity we measured the capacitance and sample thickness to determine a dielectric constant of $3.1\pm0.1$. With this dielectric constant our sample thickness was calculated to be 110 nm. The maximum modulation voltage applied was 7.3 V rms at 1 kHz providing a modulation electric field of $6.6\times10^5$ V/cm.

The experimental arrangement for the two-photon absorption experiment has been described previously.[18] The light from the dye laser was first passed through a monochromator to eliminate amplified spontaneous emission which sometimes became a problem near the limits of a dye's wavelength range. A portion of each light pulse was reflected into a photodiode to measure its intensity. The intensity of the fluorescent light from the sample, excited by two-photon transitions, was measured with a photomultiplier after passing through a second monochromator which was set to pass the peak of the fluorescent line. The signals from the photodiode and the photomultiplier were integrated with a boxcar gated integrator and the intensity of each fluorescent light signal was normalized by dividing it by the square of the signal from the photodiode. At a given wavelength the signal was averaged over 1000 laser pulses.

### III. EXCITED STATES OF PMPS

The photoconductivity and linear absorption of PMPS films[24] are shown in Fig. 1. The magnitude of the absorption coefficient shown results from the determination[20] that $\alpha$ is $4.8\times10^5$ cm$^{-1}$ at 337 nm. The exciton peak at 3.7 eV reflects the absorption of all $(Si)_n$ segments in the amorphous sample. The fluorescence maximum of 3.51 eV (Ref. 16) for PMPS films provides a better estimate for the one-photon gap $E_g$ of the longest segments. The upper bound on Stokes shifts is currently about 0.01 eV.[16,17] The distribution of segment lengths and other inhomogeneities produces a broadening of 0.3–0.4 eV in Fig. 1 to the high-energy side of $E_g=3.5$ eV.

The photoconductivity data from an earlier paper[20] in Fig. 1 parallel the optical absorption for $3.25<\hbar\omega<4.13$ eV. As discussed there, the data indicate that carriers are created by excitons diffusing to the vicinity of the surface of the film and injecting carriers from the electrode or polymer surface. To obtain the interband gap $E_b$, we measured the carrier-generation quantum efficiency for photon energies from 3.65 to 5.65 eV, as shown in Fig. 1. The strong linear increase extrapolates back to $E_b=4.6$ eV. The quantum efficiency for carrier generation in the energy range 3.5–4.0 eV was found to be lower in these experiments than that reported earlier,[20] presumably because a different electrode material was used and these experiments were conducted in a vacuum rather than in air. For Fig. 1 the earlier data were normalized to the present data at 3.75 eV.

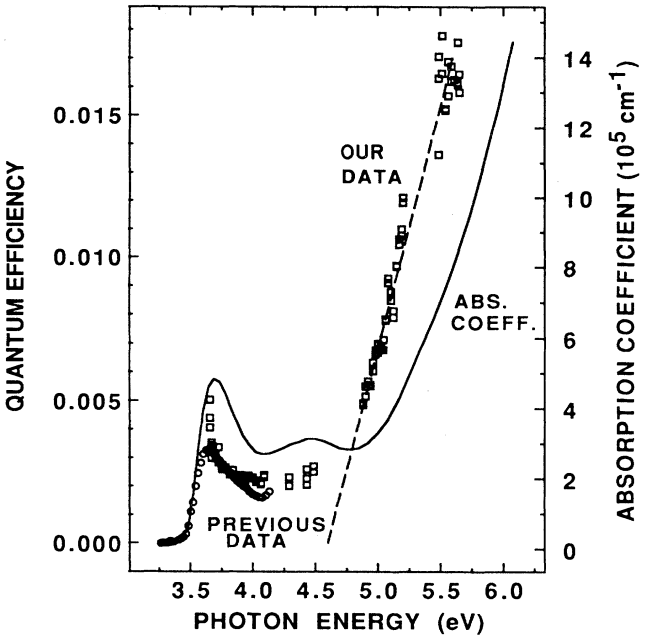


FIG. 1. The quantum efficiency for charge-carrier generation in thin PMPS films as a function of photon energy (open squares). The dashed line is a linear extrapolation of the high-energy data to 4.6 eV. The absorption coefficient (solid line) is shown for reference. The open circles are data from a previous publication (Ref. 20) normalized to the present data at 3.75 eV.

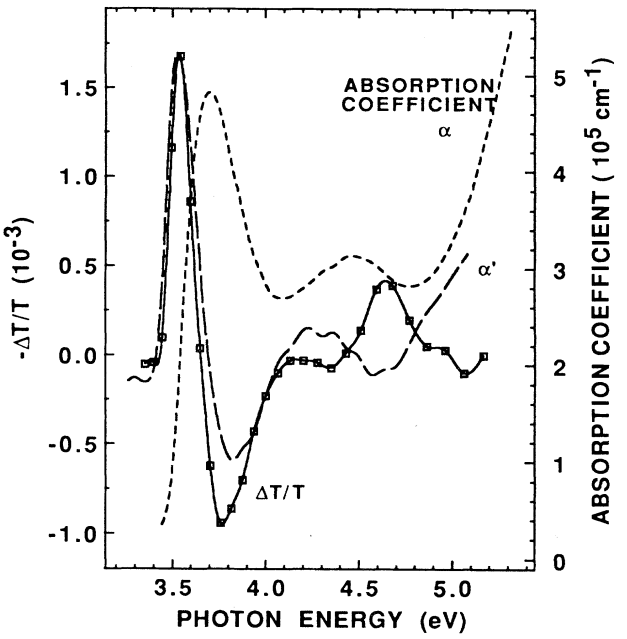


FIG. 2. The electroabsorption spectrum at room temperature of a thin PMPS film (open squares). The solid line through the open squares is to guide the eye. The absorption coefficient and the derivative of the absorption coefficient are shown as the short-dashed and long-dashed lines, respectively.

EA spectra of PMPS films at 295 and 95 K are shown in Figs. 2 and 3. $\Delta T$ is the change in transmission due to the electric field and $T$ is the transmission. The absorption spectrum $\alpha(\omega)$ of a PMPS thin film is included for reference in Fig. 2. The dashed line (long dashes) is the first derivative, $\alpha'(\omega)$, normalized to the EA spectrum at 3.54 eV. It clearly mimics the low-energy EA feature. In Fig. 3 both the 295- and 95-K spectra are shown to indicate the different behavior of the two EA features. As shown in Fig. 4, both prominent EA features vary quadratically with applied field.

The blue shift of 0.05 eV of the low-energy EA feature in Fig. 3 on cooling is also seen in the absorption spectrum[28] and provides additional evidence for associating the signal to excitons. The 4.65-eV feature does not appear to shift with temperature. In view of the interband gap of 4.6 eV obtained from photoconductivity, the 4.65-eV EA feature in Fig. 3 is assigned to be $E_b$.

Sebastian, Weiser, and Bässler[29] have summarized the analysis of Stark shifts of singlet excitons in molecular crystals. Both first and second derivatives of the linear absorption $\alpha(\omega)$ are possible, depending on the polarizability $p$ and dipole moments of the states. An $\alpha'(\omega)$ spectrum is associated with a polarizability change $\Delta p$ between the ground state $|G\rangle$ and the excited state $|^1B_u\rangle$ for polysilanes. The EA spectra in Figs. 2 and 3 show the excited state to be more polarizable, as is usually the case, since there is increased (decreased) absorption below

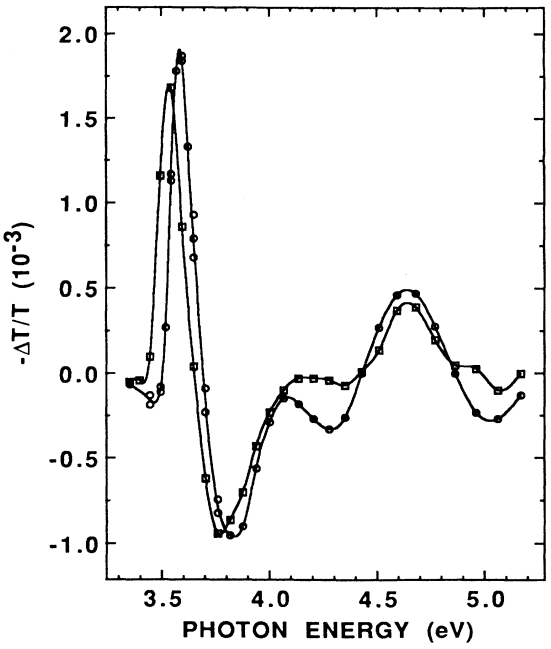


FIG. 3. The electroabsorption spectra of PMPS films at room temperature (squares) and at 95 K (circles).

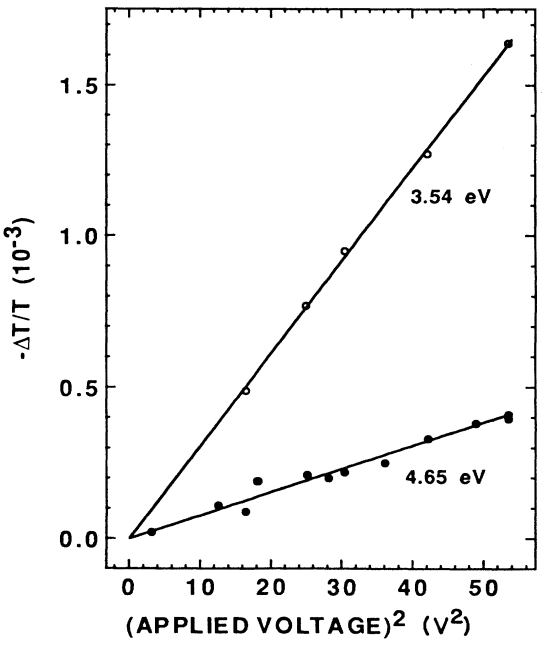


FIG. 4. The magnitude of the peak room-temperature electro-absorption signals vs the square of the applied electric field. Open circles are used for the 3.54-eV data and solid circles for the 4.65-eV data.

(above) $E_g$. The asymmetry of the EA signal around $E_g=3.7$ eV indicates small $\alpha''(\omega)$ contributions, as discussed in connection with excitons in PDA crystals.[30]

For our experiment the electric field was applied parallel to the direction of propagation of the light beam and the polymer molecules are randomly oriented in the film. When we average over all orientations of the molecules and assume that $\Delta p$ and the transition dipole moment are parallel to the $(Si)_n$ backbone, we find for the change in the absorption coefficient for the exciton

$$\Delta\alpha=\tfrac{1}{10}\Delta p F^2\frac{\partial\alpha}{\partial E}\ . \tag{1}$$

From these results we have calculated that $\Delta p$ for the first electronic transition is $1.8\times10^{-22}$ cm$^3$, a reasonable value when compared to the values obtained for molecular crystals.[29,31]

The delocalized $\sigma$ electrons along the $(Si)_n$ backbone are expected to provide the largest contribution to the polarizability difference $\Delta p$. Such contributions may be obtained exactly[32] for PPP models chosen to fit the one- and two-photon gaps of short segments. We retain all-trans segments with the actual bond lengths, an on-site repulsion $V(0)=9.04$ eV for two electrons in the same $sp^3$ orbitals, and vicinal and geminal transfer integrals $t(1\pm\delta)$, respectively, with $t=-2.40$ eV and $\delta=\frac{1}{3}$. As indicated in Table I, the exciton or $|1\,^1B_u\rangle$ state is more polarizable than the ground state $|G\rangle$. The saturation of $\Delta p(n)$ with increasing $n$ is expected on general grounds,[33] since the correlation length of alternating chains goes as $1/\delta$ and the alternation is large.

Thus $n\sim20$ is already close to an infinite chain, as indicated by various spectroscopic estimates.[9,34,35] The fit to

$$\Delta p(n)=\Delta p(\infty)+\frac{a}{n}+\frac{b}{n^2} \tag{2}$$

leads to $\Delta p(\infty)=165$ Å$^3$ for either $n=4,5,6$ or $5,6,7$ and shows $\Delta p(20)$ to be within a few percent of $\Delta p(\infty)$. Other extrapolations are possible, however. Results to $n=7$ in Table I indicate that $\Delta p(\infty)$ exceeds 100 Å$^3$, which is consistent with the experimental value of 180 Å$^3$. Smaller $\delta\sim0.15$ and $E_g\sim2$ eV in PDA leads to greater delocalization and to an order-of-magnitude larger $\Delta p$ obtained from the EA of the exciton.[30]

In organic molecular crystals, the EA signature of CT states is a second-derivative, or $\alpha''(\omega)$, curve.[29,31] The PMPS signal at 4.65 eV has the *opposite* phase, indicative of increased absorption at the center, and can be fit to $-\alpha''(\omega)$ for a hypothetical Gaussian feature

TABLE I. Polarizability, in Å$^3$, of PPP models for $(Si)_n$ segments.

| $n$ | $p(G)$ | $p(1\,^1B_u)$ | $\Delta p=p(1\,^1B_u)-p(G)$ | $p(1\,^3B_u)$ |
|---|---|---|---|---|
| 4 | 9.776 | 35.22 | 25.44 | 15.95 |
| 5 | 14.89 | 53.85 | 38.96 | 26.28 |
| 6 | 20.48 | 72.34 | 51.96 | 37.26 |
| 7 | 26.38 | 89.61 | 63.23 | |

$$\alpha(\omega)=\alpha_0\exp-(\hbar^2/\gamma^2)(\omega-\omega_0)^2 \quad (3)$$

with $\gamma=0.31$ eV. The observed EA is also inconsistent with an interband transition in a wideband semiconductor.[36] As discussed by Tokura and co-workers,[19,37] field-induced transitions to even-parity $A_g$ states can appear as an enhanced EA signal. We will return to the 4.65-eV signal after showing that it does not correspond to an $^1A_g$ excited state.

The idealized all-trans $(Si)_n$ backbone has inversion symmetry in infinite chains. The TPA spectra of PMPS films, shown in Fig. 5 on a logarithmic scale, then identify some of the even-parity states of the polymer. The low-energy TPA around 4.4 eV is slightly blue shifted at 11 K, just as are the linear and EA signals on cooling. In the more ordered PDHS, whose TPA at 11 K (Ref. 18) is shown in Fig. 6 along with that of PMPS on a linear scale, the sharp TPA shifts from 4.18 eV at 295 K to 4.27 eV at 11 K, while the widths at half height decrease from $\sim 0.2$ to $<0.1$ eV.[18] We consequently retain the PPP description of TPA in PDHS and consider the role of disordered side groups in PMPS.

The alternation gap $E_a$ to the second $^1A_g$ state is slightly above $1.2E_g$ in PPP models with polysilane parameters,[8] with little dependence on the segment length $n$. Although the one-photon gap $E_g$ decreases with $n$ up to $n\sim 20$, the similar behavior of the two-photon gap $E_a$ leads to an essentially constant ratio. The longest PMPS segments have $E_g=3.51$ eV, as obtained from fluorescence, and thus have $E_a$ slightly above 4.2 eV. The 0.3–0.4 eV width of the exciton peak in Fig. 1 produces a similar broadening of the alternation gap and accounts for the broad TPA from 4.3 to 4.6 eV in Fig. 5 without introducing additional parameters.

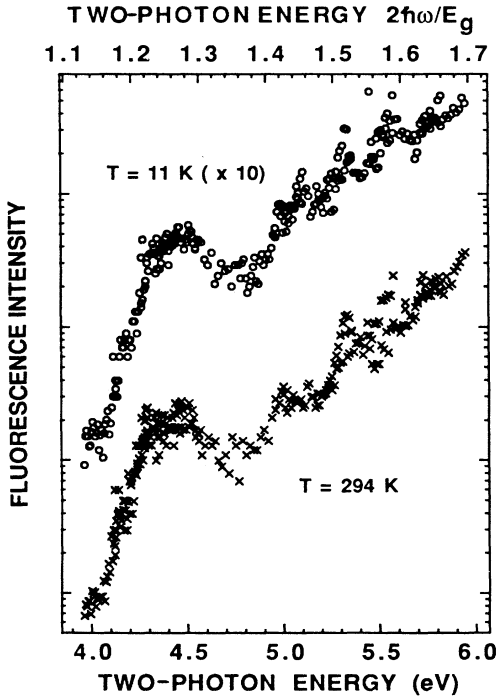


FIG. 5. The two-photon absorption spectrum on a logarithmic scale of thin solid films of PMPS as determined from the fluorescence intensity vs two-photon energy. The ×'s are the data obtained at room temperature and the open circles are the data (×10) obtained at 11 K.

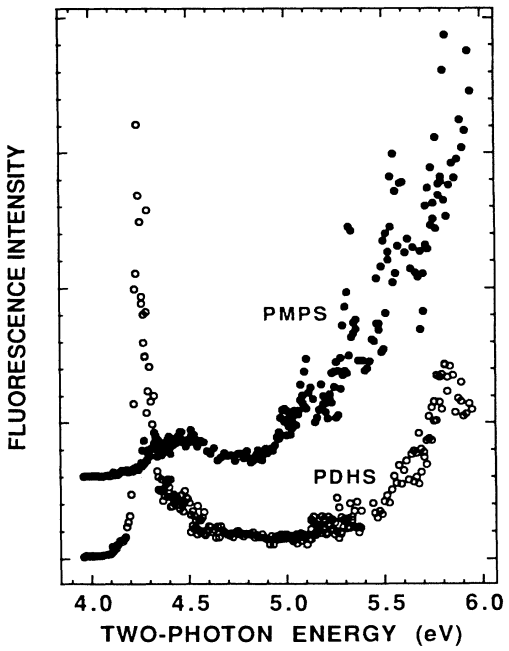


FIG. 6. The 11-K two-photon absorption spectrum on a linear scale of poly(methylphenylsilane) (solid circles) and of poly(di-*n*-hexylsilane) (open circles), from Ref. 18. The baselines for the two sets of data are offset for clarity.

The broad TPA above 5 eV is assigned to an even-parity state derived from exciting two electrons across $E_g$. As discussed[18] for the similar PDHS feature in Fig. 6, the TPA intensity is an order of magnitude higher for the high-energy feature around $1.78E_g$ for silicon parameters in the PPP model. Even in PDHS, the width exceeds 1 eV, the maximum could not be found, and short excited-state lifetime rather than disorder is indicated. Disorder broadening of 0.3–0.4 eV in PMPS hardly affects such a broad line and the high-energy features of PMPS and PDHS in Fig. 6 are similar. We note, however, that the 12-fold intensity increase of the TPA in PDHS between 295 and 11 K is completely absent in PMPS and that its high-energy TPA appears to be shifted to slightly lower rather than higher energy. At this stage, the PPP model for $\sigma$ conjugation is quite qualitative and does not explicitly include side groups or conformational changes.

In addition to the one-photon gap $E_g$, the alternation gap $E_a$, and the interband gap $E_b$, polysilanes are expected to have a gap $E_t$ to the lowest triplet state. Phosphoresence has recently been reported in

TABLE II. Exact PPP excitation energies (eV) of $(Si)_n$ segments with $n=4$, 5, 6, and 7, alternation $\delta=\frac{1}{3}$, $t=-2.40$ eV, and $V(0)=9.04$ eV.

| $n$ | $E_g$ | $E_a$ | $E_t$ |
|---|---|---|---|
| 4 | 5.328 | 6.393 | 4.089 |
| 5 | 4.931 | 5.986 | 3.875 |
| 6 | 4.673 | 5.747 | 3.755 |
| 7 | 4.493 | 5.596 | 3.682 |

poly(methylpropylsilane)[38] and in PDHS.[39] In both cases, temperatures below $\sim 20$ K are required and $E_t$ is only some 0.10–0.15 eV below the flourescence, which as already noted is at $E_g$ when Stokes shifts are negilgible. For completeness, we have extended the PPP model to the lowest triplet, $|1\,^3B_u\rangle$, of $(Si)_n$ to $n=7$ and have also calculated its static polarizability. The resulting excitation energies are listed in Table II, along with previous results for $E_g$ and $E_a$. The difference between $E_g$ and $E_t$ decreases with increasing $n$, as expected for increasing delocalization. The value of $E_g-E_t$ in infinite chains may be obtained by extrapolating against $1/n$ or according to Eq (2). The ratio $E_t/E_g$ in Table II increases from 0.7632 at $n=4$ to 0.8195 at $n=7$. The triplet is estimated to be $\sim 0.4$ eV below $E_g$ in the infinite chain.

PPP models for hydrocarbons have transferable parameters that typically reproduce excitation energies to better than 0.5 eV. The estimated $E_g-E_t$ of 0.4 eV is consequently in reasonable agreement with the smaller experimental values of 0.15 eV in[38] poly(methylpropylsilane) and 0.12 eV in[39] PDHS. Table I shows the singlet exciton to be far more polarizable than the triplet; $|1\,^1B_u\rangle$ is an ionic state, while $|G\rangle$ and $|1\,^3B_u\rangle$ are covalent and have similar polarizabilities. Thus $E_g$ is stabilized more than $E_t$ in a solid-state environment and $E_g-E_t$ is reduced.

## IV. DISCUSSION

Except for the triplet gap $E_t$, all the excitation energies obtained above are for similarly prepared PMPS films. Comparison of linear absorption, flourescence, electroabsorption, photoconductivity, and two-photon absorption is then more direct. To the extent that all polysilanes illustrate $\sigma$ conjugation, on the other hand, their excitation energies are also comparable. To a first approximation, variations in segment lengths between ordered and amorphous systems can be included by relating all excitation energies to the one-photon gap $E_g$ for the longest segments. Since Stokes shifts are negligible, $E_g$ may be obtained in either absorption or emission.

The energy spectrum of $(Si)_n$ segments with $n\sim 20$ is extremely dense, even in models restricted to the half-filled $\sigma$-conjugated backbone. Band edges associated with alternation, with singlet excitons, or with charge carriers are most likely to be observed experimentally and have been designated as $E_a$, $E_g$, and $E_b$, respectively. As shown by the TPA spectra in Fig. 5, however, other groups of states may also contribute. The assignment of all features in EA or linear spectra is rarely possible. The excitations of conjugated molecules, or of short $(Si)_n$ segments, may be obtained using PPP models and provide some guidance for interpreting polymer spectra.

EA spectra are both sensitive and difficult to assign. Various connections to the linear absorption spectrum, $\alpha(\omega)$, have been discussed. Stark shifts of discrete levels lead to $\alpha'(\omega)$ features, as shown by the exciton feature in Fig. 3; the broadening of CT transitions in molecular solids leads to $\alpha''(\omega)$ features;[29,31] in the low-field regime, when lifetime broadening dominates, wideband semiconductors show $\alpha''(\omega)$ curves.[40] An entirely different set of EA signals[37] is due to even-parity states that become allowed at finite field $F$. Crystalline PDA-PTS (PTS represents $p$-toluene sulfonate) has[41] such an EA feature[42] in the transparent regime well below $E_g$. Transitions to even-parity states in regions with finite $\alpha(\omega)$ may show Fano-type resonances.[19] Independent knowledge of the linear spectrum and of the photoconductivity was used to assign the $E_g$ and $E_a$ features of PMPS in Fig. 3.

The photoconductivity data suggest that the 4.65-eV feature in Fig. 3 is related to CT between $(Si)_n$ segments in amorphous PMPS. Without attempting a microscopic model, we consider a transfer integral $t'<t$ between the terminal sites of segments with $n=p$ and $q$. The ground state for small $t'$ is a product function $|G_pG_q\rangle$ and the excited states are hardly shifted. CT excitations to $|p^+q^-\rangle$ or $|p^-q^+\rangle$ are now possible, however, and their intensity is roughly $(t'/t)^2$ less than intrasegment excitations. The electron-hole ($e$-$h$) symmetry[8] of half-filled PPP or extended Hubbard models leads to degenerate $|p^+q^-\rangle$ and $|q^-q^+\rangle$ states in the limit $t'=0$. For small $t'$, $e$-$h$ selection rules lead to CT between $|G_pG_q\rangle$ and the odd linear combination, $|p^+q^-\rangle-|p^-q^+\rangle$. The even linear combination is dipole forbidden and shifted to higher energy due to configuration interaction with $|G_pG_q\rangle$ and other states with even $e$-$h$ symmetry.

The $F=0$ absorption spectrum thus contains intersegment CT transitions to states with odd $e$-$h$ symmetry, for any relative orientation of PPP segments of length $p$ and $q$. A static field $F>0$ mixes states of opposite $e$-$h$ symmetry and strongly couples nearly degenerate ion pairs on adjacent segments. CT intensity for $F>0$ is transferred from allowed to forbidden transitions at $F=0$. The $-\alpha''(\omega)$ fit for the 4.65-eV feature in Fig. 3 is based on Eq. (3) and is consistent with unchanged overall absorption, increased $\alpha(\omega)$ at 4.65 eV, and reduced $\alpha(\omega)$ at lower energy. We have yet to rationalize the symmetric decrease on the high-energy side, however, and the proposed connection between EA and intersegment CT in PMPS is preliminary.

Tachibana *et al.*[19] have reported a Stark-shifted exciton at $E_g=3.4$ eV in the EA spectrum of PDHS at 77 K. They also observed an EA signal at $E_a=4.22$ eV that matches the TPA in Fig. 6 and an intense EA signal above 5 eV. Thus $E_a$ but not $E_b$ is observed in PDHS films, while the opposite holds for PMPS films. Our applied field of $6.6\times 10^5$ V/cm is about twice as large as theirs, at $3.8\times 10^5$ V/cm. The ordered side groups in

PDHS and the disordered side groups in PMPS evidently lead to quite different EA spectra. Since all features go as $F^2$, the exciton in Fig. 3 is quite consistent with a doubling of the PMPS linewidth to $2\Gamma(^1B_u)\sim 0.2-0.3$ eV. Such an energy distribution, which has already been invoked in connection with the absorption and fluorescence, interferes with any weak signal above $E_g$.

The observation of an EA signal at $E_a$ due to the admixing of odd-parity states in $|2\,^1A_g\rangle$ depends on the segment distribution. The sharp TPA in Fig. 6 for PDHS at 11 K is at least five times narrower than the PMPS signal. EA at $E_a$ is reduced correspondingly or even more, if there are interference effects, and detection becomes marginal even at higher fields. A broad distribution of segments thus makes it more difficult to resolve even-parity states of individual segments. Together with the broader excitonic feature, this rationalizes the absence of an EA signal at $E_a$ in PMPS.

The interband gap $E_b$ presumably reflects ionization of the longest segments, as well as charge motion between segments and between polymeric strands. The long segments in PDHS and shorter segments in PMPS lead to similar junctions between segments, unless the segments are also postulated to be ordered. The more numerous junctions between shorter segments enhance intersegment CT, while the width of such processes need not depend strongly on segment length. The $(F_2/F_1)^2$ dependence of EA reduces our 4.65-eV feature to $\sim 10^{-4}$ at $F_1 = 3.8\times 10^5$ V/cm and such weak features were not assigned by Tachibana *et al.*[19] The experimental identification of $E_b$ in PDHS films is in progress.

We emphasize here the potentially different manifestations of segment distributions for various EA features. The connection of the interband gap $E_b$ to the electronic structure of individual segments, whether in PPP, Hubbard, Hückel, or other models, also remains to be found. The ionization potential or electron affinity can be obtained for finite segments. Unlike the neutral excitations involving $E_a$, $E_t$, or $E_g$, however, charge carriers are known to interact strongly with the medium and polarization energies around an eV per charge are typical in organic solids.[43] Thus $E_b$ may be more sensitive to side groups and to chain conformation. The identification of the excitation energies $E_g$, $E_a$, $E_b$, and $E_t$ in other polysilanes, with various segment distributions and side groups, is clearly needed.

## V. CONCLUDING REMARKS

The excitation energies $E_g$, $E_a$, and $E_b$ of PMPS films, as well as the singlet-triplet gap $E_t$ of other polysilanes, have much in common with excitations of organic molecular crystals such as anthracene. Ordered regions of the $\sigma$-conjugated backbone, or segments, play the role of molecules. Wideband semiconductors provide fewer connections, in spite of the occurrence of half-filled bands, because electron-electron correlations are strong enough to lead to excitons in these one-dimensional systems. The gap between the valence and conduction bands, which dominates the response of wideband systems, may perhaps be associated with the direct generation of charge at $E_b$, although the EA signal has the opposite phase and has been suggested to be CT between segments. The experimental determination of different excitation energies in PMPS films should facilitate more quantitative modeling of $(Si)_n$ segments. We have also touched on the role of side-group order by contrasting amorphous PMPS and more crystalline PDHS.

We note, in summary, that the PPP description of the PMPS excited states provides a general qualitative picture for the electronic structure of $(Si)_n$ segments. More quantitative assignments of EA, TPA, photoconduction, and other features, on the other hand, should reveal differences among various systems associated with side-group and conformational contributions. Both the general problem of $\sigma$ conjugation in polysilanes and the understanding of specific systems can be addressed by obtaining the excitation energies of other polysilanes, and such studies are in progress.

## ACKNOWLEDGMENTS

The technical assistance of P. M. Beeson and P. C. M. McWilliams is gratefully acknowledged. The work at Sandia National Laboratories was supported by the U.S. Department of Energy under Contract No. DE-AC04-76DP00789 and the work at Princeton University was partially supported by NSF Grant No. NSF-DMR-8921072.

[1]Proceedings of the International Conference on the Science and Technology of Synthetic Metals, Santa Fe, N. M. 1988 [Synth. Metals **27** (1988); **28** (1989); **29** (1989)].

[2]*Conjugated Polymeric Materials: Opportunities in Electronics, Optoelectronics, and Molecular Electronics,* Vol. 182 of NATO Advanced Study Institute, Series E, edited by J. L. Brédas and R. R. Chance (Kluwer, Dordrecht, 1990).

[3]*Nonlinear Optical Properties of Organic Molecules and Crystals,* edited by D. S. Chemla and J. Zyss (Academic, New York, 1987), Vols. 1 and 2.

[4]*Nonlinear Optical and Electroactive Polymers,* edited by P. N. Prasad and D. R. Ulrich (Plenum, New York, 1988).

[5]D. R. Ulrich, Mol. Cryst. Liq. Cryst. **189**, 3 (1990).

[6]M. Pope and C. E. Swenberg, *Electronic Processes in Organic Crystals* (Clarendon, Oxford, 1982).

[7]A. J. Heeger, S. Kivelson, J. R. Schrieffer, and W. P. Su, Rev. Mod. Phys. **60**, 781 (1988).

[8]Z. G. Soos and G. W. Hayden, Chem. Phys. **143**, 199 (1990).

[9]R. D. Miller and J. Michl, Chem. Rev. **89**, 1359 (1989).

[10]L. A. Harrah and J. M. Zeigler, in *Photophysics of Polymers,* edited by C. E. Hoyle and J. M. Torkelson (American Chemical Society, Washington, DC, 1987).

[11]C. Sandorfy, Can. J. Chem. **33**, 1337 (1955).

[12]G. C. Pitt, in *Homoatomic Rings, Chains, and Macromolecules of Main-Group Elements,* edited by A. L. Reingold (Elsevier, Amsterdam, 1977).

[13]M. R. Philpott, Chem. Phys. Lett. **50**, 18 (1977).
[14]J. R. G. Thorne, Y. Ohsako, J. M. Zeigler, and R. M. Hochstrasser, Chem. Phys. Lett. **162**, 455 (1989).
[15]K. S. Schweizer, Synth. Metals **28**, C565 (1989).
[16]A. Elschner, R. F. Mahrt, L. Pautmeier, H. Bässler, and M. Stolka, Chem. Phys. **150**, 81 (1991).
[17]H. P. Trommsdorff, J. M. Zeigler, and R. M. Hochstrasser, J. Chem. Phys. **89**, 4440 (1988).
[18]Z. G. Soos and R. G. Kepler, Phys. Rev. B **43**, 11 908 (1991).
[19]H. Tachibana, Y. Kawabata, S.-y. Koshihara, and Y. Tokura, Solid State Commun. **75**, 5 (1990).
[20]R. G. Kepler, J. M. Zeigler, L. A. Harrah, and S. R. Kurtz, Phys. Rev. B **35**, 2818 (1987).
[21]R. G. Kepler and J. M. Zeigler, in *Silicon-Based Polymer Science: A Comprehensive Resource,* edited by J. M. Zeigler and F. W. G. Fearon (American Chemical Society, Washington, DC, 1990).
[22]R. G. Kepler and J. M. Zeigler, Mol. Cryst. Liq. Cryst. **175**, 85 (1989).
[23]M. A. Abkowitz, M. J. Rice, and M. Stolka, Philos. Mag. B **61**, 25 (1990).
[24]R. G. Kepler and J. M. Zeigler, in *Advanced Organic Solid State Materials,* edited by L. Y. Chiang, P. L. Chaikin, and D. O. Cowan, MRS Symposia Proceedings, No. 173 (Materials Research Society, Pittsburgh, 1990).
[25]R. G. Kepler, Polym. Prep. Am. Chem. Soc. Div. Polym. Chem. **31**, 287 (1990).
[26]R. G. Kepler and Z. G. Soos, in Proceedings of the International Conference on Synthetic Metals (ICSM 90), Tubingen, 1990 [Synth. Metals **41-43**, 1543 (1991)].
[27]J. M. Zeigler, Polym. Prepr. Am. Chem. Soc. Div. Polym. Chem. **27**, 109 (1987).
[28]R. G. Kepler (unpublished).
[29]L. Sebastian, G. Weiser, and H. Bässler, Chem. Phys. **61**, 125 (1981).
[30]L. Sebastian and G. Weiser, Chem. Phys. **62**, 447 (1981).
[31]L. Sebastian, G. Weiser, G. Peter, and H. Bässler, Chem. Phys. **75**, 103 (1983).
[32]Z. G. Soos and G. W. Hayden, Phys. Rev. B **40**, 3081 (1989).
[33]Z. G. Soos, S. Kuwajima, and J. E. Mihalick, Phys. Rev. B **40**, 3124 (1985).
[34]L. A. Harrah and J. M. Zeigler, Macromolecules **20**, 601 (1987).
[35]P. Trefonas, R. West, R. D. Miller, and D. Hofer, J. Polym. Sci., Polym. Lett. Ed. **21**, 823 (1983).
[36]D. F. Blossey and P. Handler, in *Semiconductors and Semimetals,* edited by R. K. Willardson and A. C. Beer (Academic, New York, 1972).
[37]Y. Tokura, Y. Oowaki, T. Koda, and R. H. Baughman, Chem. Phys. **88**, 437 (1984).
[38]O. Ito, M. Terazima, and T. Azumi, J. Am. Chem. Soc. **112**, 444 (1990).
[39]C. Walsh, W. P. Ambrose, D. M. Burland, R. D. Miller, and D. S. Tinti (unpublished).
[40]D. E. Aspnes and J. E. Rowe, Phys. Rev. B **5**, 4022 (1972).
[41]S. Etemad and Z. G. Soos, in *Advances in Spectroscopy: Spectroscopy of Advanced Materials,* edited by R. J. H. Clark and R. E. Hester (Wiley, New York, in press).
[42]L. Sebastian and G. Weiser, Chem. Phys. Lett. **64**, 396 (1979).
[43]F. Gutman and L. E. Lyons, *Organic Semiconductors* (Wiley, New York, 1967), p. 342.